
CXPlain: Causal Explanations for Model Interpretation under Uncertainty

Patrick Schwab and Walter Karlen

Institute of Robotics and Intelligent Systems, ETH Zurich
patrick.schwab@hest.ethz.ch

Abstract

Feature importance estimates that inform users about the degree to which given inputs influence the output of a predictive model are crucial for understanding, validating, and interpreting machine-learning models. However, providing fast and accurate estimates of feature importance for high-dimensional data, and quantifying the uncertainty of such estimates remain open challenges. Here, we frame the task of providing explanations for the decisions of machine-learning models as a causal learning task, and train causal explanation (CXPlain) models that learn to estimate to what degree certain inputs cause outputs in another machine-learning model. CXPlain can, once trained, be used to explain the target model in little time, and enables the quantification of the uncertainty associated with its feature importance estimates via bootstrap ensembling. We present experiments that demonstrate that CXPlain is significantly more accurate and faster than existing model-agnostic methods for estimating feature importance. In addition, we confirm that the uncertainty estimates provided by CXPlain ensembles are strongly correlated with their ability to accurately estimate feature importance on held-out data.

1 Introduction

Explanation methods for machine-learning models play an important role in researching, developing, and using predictive models as information on what features were important for a given output enable us to better understand, validate, and interpret model decisions [1–5]. However, complex models, such as ensemble models and deep neural networks, are often difficult to interrogate. To address this apparent dichotomy between performance and interpretability [6], researchers have developed a number of attribution methods that provide estimates of the importance of input features towards a model’s output for specific types of models [4, 7–15], and for any machine-learning model [6, 16].

However, providing fast and accurate feature importance estimates for any machine-learning model is challenging because there exists a wide variety of intricate machine-learning models with different underlying model structures, algorithms, and decision functions, which makes it difficult to develop an optimised and unified approach to importance attribution. Furthermore, importance estimates of state-of-the-art methods are typically associated with significant uncertainty [3, 17–19], and it is therefore difficult for users to judge when importance estimates can be expected to be accurate.

In this work, we present a new approach to estimating feature importance for any machine-learning model using causal explanation (CXPlain) models. CXPlain uses a causal objective to train a supervised model to learn to explain another machine-learning model. This approach can be applied to any machine-learning model, since it has no requirements on the predictive model to be explained. In particular, it does not require retraining or adapting the original model. We demonstrate experimentally that CXPlain is significantly more accurate than most existing methods, fast, and able to produce accurate uncertainty estimates. Source code is available at <https://github.com/d909b/cxplain>.

Contributions. This work contains the following contributions:

- We introduce causal explanation (CXPlain) models, a new method for learning to accurately estimate feature importance for any machine-learning model.
- We present a methodology based on bootstrap resampling for deriving uncertainty estimates for the feature importance scores provided by CXPlain.
- Our experiments show that CXPlain is significantly more accurate and significantly faster (at evaluation time) than existing model-agnostic methods, and that the uncertainty estimates for its assigned feature importance scores are strongly correlated with the accuracy of the provided importance scores on previously unseen test data.

2 Related Work

Feature Importance Estimation. Existing methods for feature importance estimation can be subdivided into (1) gradient-based methods, (2) methods based on sensitivity analysis, (3) methods that measure the change in model confidence when removing input features, and (4) mimic models. Simple Gradient (SG) [8], Integrated Gradients (IG) [10], DeepLIFT [1], and DeepSHAP [6] are examples of gradient-based methods. Gradient-based methods are only applicable to differentiable models, such as neural networks, and their computation is typically fast. Methods that quantify a model’s sensitivity to changes in the input, such as LIME [16] or SHAP [6], and more specifically Kernel SHAP, are applicable to any machine-learning model but typically slow to compute, as large numbers of model evaluations are necessary to assess a model’s sensitivity. Methods based on masking parts of the input and measuring the model’s resulting change in confidence [20] include conditional multivariate models for visualising deep neural networks [21], analysing the effects of erasing parts of their representations [22], image interpretation by identifying the regions for which the model most strongly responds to perturbations [23], and image masking models trained to manipulate the outputs of a predictive model by occluding parts of the input [24]. The fourth main category of approaches to explaining model decisions is to train interpretable models that mimic the decisions of a black-box model that we wish to explain. Tree- [25–27] and rule-based [28] models have been used as mimic models. However, mimic models are not guaranteed to match the behavior of the original model. Besides these four established categories of feature importance estimation methods, structural causal models (SCMs) [29] and Deep Taylor Decomposition (DTD) [30] have also recently been proposed as explanation methods. However, these methods are designed for specific types of models. In addition, the L2X method that uses a variational approximation of mutual information [31] and Bayesian nonparametrics [32] have been proposed to explain a target model. Tsang et al. [33] detected statistical interactions by interpreting the weights learned in neural networks. Beyond feature attribution, testing with concept activation vectors (TCAV) [34] was proposed to visualise the internal state of deep learning models, and influence functions [35] have been used to identify the training data most responsible for a given model decision. A major limitation of most existing methods for feature importance estimation is that they do not inform users when their estimates are significantly uncertain and can not be expected to be accurate.

Uncertainty and Reliability of Explanations. Although reliability is necessary for model explanations to be trustworthy, relatively few studies have been concerned with quantifying the uncertainty and robustness of explanation methods. For example, it has been shown that multiple importance estimation methods incorrectly attribute when a constant vector shift is applied to the input [3], that the attributions provided by interpretation methods may themselves contain significant uncertainty [18], that some explanation methods are independent of both the model and the data-generating process and, thus, can not be relied upon for important interpretation tasks [17], and that imperceptibly small perturbations of the input can significantly alter the explanations provided by state-of-the-art

Table 1: Comparison of CXPlain to several representative methods for feature importance estimation.

	CXPlain	SG [8] / IG [10]	DeepSHAP [1, 6]	LIME [16]	SHAP [6]
Accuracy	high	moderate	high	high	high
Model-agnostic	✓	×	×	✓	✓
Uncertainty estimates	✓	×	×	×	×
Computation time	fast	fast	fast	slow	slow

explanation methods without changing the explained model’s prediction [19]. These studies highlight the importance of informing users when a given explanation is uncertain and should be discounted.

In contrast to existing works, CXPlain is an explanation model trained with a causal objective to learn to explain the decisions of any machine-learning model without the need to retrain, adapt, or have in-depth knowledge of the explained model. To the best of our knowledge, CXPlain is the first feature importance estimation method that is simultaneously (1) significantly more accurate than most existing methods, (2) compatible with any machine-learning model and data modality, (3) able to provide uncertainty estimates via bootstrap resampling, and (4) fast at evaluation time (Table 1).

3 Methodology

Problem Setting. We consider a setting in which we are given a predictive model \hat{f} which processes inputs X consisting of p input features, or groups of features, x_i with $i \in [0 \dots p - 1]$ to produce outputs $\hat{y} \in \mathbb{R}^k$ of any dimensionality k . The predictive model \hat{f} is scored according to an objective function $\mathcal{L} : y \times \hat{y} \rightarrow s$ that computes a scalar loss $s \in \mathbb{R}$ after comparing the model’s predictive output \hat{y} to a ground-truth output $y \in \mathbb{R}^k$. The mean squared error (MSE) for regression models and the categorical crossentropy for classification models are commonly used examples of such objectives. We note that we specifically do not require access to, or knowledge of, the process by which \hat{f} produces its output, nor do we require \hat{f} to be differentiable or of any specific form. Additionally, we are given $N \in \mathbb{N}$ independent and identically distributed (i.i.d.) pairs of sample covariates X and ground-truth outputs y as training data. Given this setting, our goal is to train an explanation model \hat{f}_{exp} that produces accurate estimates \hat{A} with elements \hat{a}_i corresponding to the importances assigned to each of the p input features x_i to the predictive model \hat{f} .

Causal Explanations (CXPlain). The main idea behind CXPlain is to train a separate explanation model \hat{f}_{exp} to explain the predictive model \hat{f} (Figure 1). This flexible framework has the advantage that we do not need to retrain or adapt the predictive model \hat{f} to explain its decisions. To train the explanation model, we utilise a causal objective function that quantifies the marginal contribution of either a single input feature or group of input features towards the predictive model’s accuracy [14, 20]. This approach, in essence, transforms the task of producing feature importance estimates for a given predictive model into a supervised learning task that we can address with existing supervised machine-learning models.

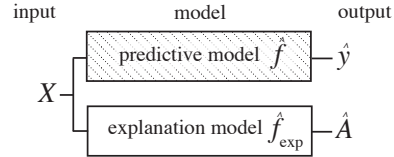


Figure 1: CXPlain trains an explanation model \hat{f}_{exp} (bottom) to learn to estimate importance scores \hat{A} for a predictive target model \hat{f} (top) given features X .

Causal Objective. The core component of CXPlain is the causal objective that enables us to optimise explanation models to learn to explain another predictive model. The causal objective we build on was first introduced to jointly learn to produce accurate predictions and estimates of feature importance in a single neural network model [14]. However, the original formulation of the causal objective required a specific attentive mixture of experts architecture. In this work, we contribute an adapted version of the causal objective from [14] that does not require a specific model structure, and that can be used to train explanation models to learn to explain any machine-learning model. The causal objective introduced in [14] was based on the Humean definition of causality used by Granger [36], who defined a causal relationship $x_i \rightarrow \hat{y}$ between random variables x_i and \hat{y} to exist if we are better able to predict \hat{y} using all available information than if the information apart from x_i had been used [14]. i.e. if the absence of x_i as a feature decreases our ability to predict \hat{y} . Granger [36]’s definition of causality was based on two key assumptions: (1) That our set of available variables X contains *all* relevant variables for the causal problem being modelled, and (2) that x_i temporally precedes \hat{y} [36]. In the general setting, these assumptions can not be verified from observational data [37]. However, in our specific setting, we know a priori that the inputs of the predictive model \hat{f} mathematically always precede its output, and that the explained model’s output, on deterministic hardware and software, is not influenced by variables other than those present in its set of input features. We can therefore use the given definition to quantify the degree to which an input feature caused a marginal improvement in the predictive performance of the predictive model

\hat{f} . Given input covariates X , we therefore denote $\varepsilon_{X \setminus \{i\}}$ as the predictive model’s error without including any information from the i th input feature and ε_X as the predictive model’s error when considering all available input features. To calculate $\varepsilon_{X \setminus \{i\}}$ and ε_X , we first compute the outputs $\hat{y}_{X \setminus \{i\}}$ and \hat{y}_X of the predictive model \hat{f} without and with the i th input feature x_i , respectively:

$$\hat{y}_{X \setminus \{i\}} = \hat{f}(X \setminus \{i\}) \quad (1) \quad \hat{y}_X = \hat{f}(X) \quad (2)$$

There are several different approaches to obtaining $X \setminus \{i\}$ from the full set of input features, depending on the type of input data. For most types of data, masking the respective input feature x_i at index i with zeroes, when the zero value has no special meaning, or replacing it with the mean value across the entire data set are both valid choices [20, 21, 24]. More sophisticated feature masking schemes that consider the masked feature’s distribution [38, 39] could be a more principled alternative to masking with point-wise estimates. Given $X \setminus \{i\}$, we compare the predictions $\hat{y}_{X \setminus \{i\}}$ and \hat{y}_X with the ground-truth labels y using the predictive model’s loss function \mathcal{L} to calculate $\varepsilon_{X \setminus \{i\}}$ and ε_X :

$$\varepsilon_{X \setminus \{i\}} = \mathcal{L}(y, \hat{y}_{X \setminus \{i\}}) \quad (3) \quad \varepsilon_X = \mathcal{L}(y, \hat{y}_X) \quad (4)$$

Following Granger [36]’s definition of causality, we define the degree $\Delta\varepsilon_i$ to which the i th input feature causally contributed to the predictive model’s output \hat{y} as the decrease in error, as measured by its loss \mathcal{L} , associated with adding that feature to the set of available information sources [14]:

$$\Delta\varepsilon_{X,i} = \varepsilon_{X \setminus \{i\}} - \varepsilon_X \quad (5)$$

Lastly, we normalise the importance scores ω_i to relative contributions $\in [0, 1]$ with $\sum_i \omega_i = 1$ [14]:

$$\omega_i(X) = \frac{\Delta\varepsilon_{X,i}}{\sum_{j=0}^{p-1} \Delta\varepsilon_{X,j}} \quad (6)$$

We then arrive at our causal objective $\mathcal{L}_{\text{causal}} = \frac{1}{N} \sum_{l=0}^{N-1} \text{KL}(\Omega_{X_l}, \hat{A}_{X_l})$ [14] that aims to minimise the Kullback-Leibler (KL) divergence [40] between the target importance distribution Ω with $\Omega(i) = \omega_i(X)$ for a given sample X , and the distribution of importance scores \hat{A} with $\hat{A}(i) = \hat{a}_i$ as estimated by \hat{f}_{exp} based on X . Using $\mathcal{L}_{\text{causal}}$, we can train supervised learning models to learn to explain any other machine-learning model based solely on its outputs, and without the need to retrain the model to be explained. Precomputing the importances Ω for each training sample X takes $N(p+1)$ evaluations of the target predictive model at training time. For high-dimensional images, it is sensible to group non-overlapping regions of adjacent pixels into feature groups, since removing single pixels in high-dimensional images is unlikely to strongly affect a predictive model’s output [21]. This also significantly limits the number of feature groups p for which importances ω_i have to be precomputed. We note that estimating \hat{A} is not necessary in situations in which ground truth labels are readily available, e.g. during model development. In those situations, Ω can directly be used to explain \hat{f} .

Explanation Models. In principle, any supervised machine learning model that can be trained with a custom objective could be used as a causal explanation model. In this work, we focus on neural explanation models. Using deep neural networks as causal explanation models has the advantage that these models are able to extract high-level feature representations from high-dimensional and unstructured data [41], and thus remove the need to perform manual feature engineering. We leave the exploration of other classes of explanation models to future work. A priori, it is not clear which architectures would be most suitable to be used in neural explanation models. Absent any prior knowledge about the structure of the input data, multilayer perceptrons (MLPs) are likely a sensible default choice. However, since architectures that exploit the spatial or temporal structure of input data have been shown to be efficacious, we reason that, depending on the data modality of the input features of the model to be explained, special-purpose architectures, such as convolutional neural networks [42] for images and attentive neural networks for texts [43], could perform better than MLPs. In particular, U-nets [44] that have been designed for image segmentation, a task that involves mapping input pixels to segmentation labels, may perform well as causal explanation models for images since segmentation is semantically similar to explanation, which involves mapping input pixels to importance scores. To determine whether or not specialised model architectures can achieve better performances in neural explanation models, we experimentally evaluate both MLPs and U-nets.

Uncertainty of Importance Estimates. In addition to producing accurate estimates of feature importance, we wish to provide uncertainty estimates u_i that quantify the uncertainty associated with each individual feature importance estimate \hat{a}_i produced by a CXPlain model. In particular, we

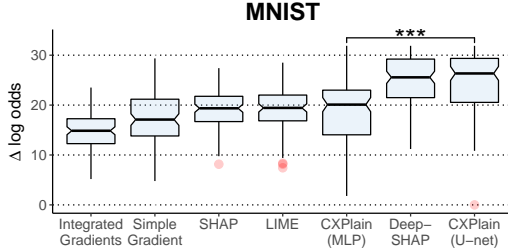


Figure 2: Comparison of the distributions of the changes in log odds $\Delta \log$ -odds after masking the top 10% most important pixels according to several feature importance estimation methods across $N = 100$ MNIST test images (higher is better). *** = significantly different ($p < 0.001$, MWW).

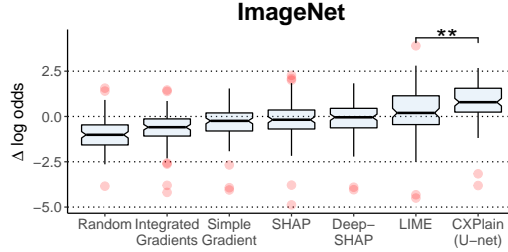


Figure 3: Comparison of the distributions of the changes in log odds $\Delta \log$ -odds after masking the top 30% most important pixels according to several feature importance estimation methods across $N = 100$ test ImageNet images (higher is better). ** = significantly different ($p < 0.01$, MWW).

would like to calculate confidence intervals $CI_{i,\gamma} = [c_{i,\frac{\alpha}{2}}, c_{i,1-\frac{\alpha}{2}}]$ with lower bounds $c_{i,\frac{\alpha}{2}}$ and upper bounds $c_{i,1-\frac{\alpha}{2}}$ at confidence level $\gamma = 1 - \alpha$ for each assigned feature importance estimate \hat{a}_i . The width $u_i = c_{i,1-\frac{\alpha}{2}} - c_{i,\frac{\alpha}{2}}$ of $CI_{i,\gamma}$ can subsequently be used to quantify the uncertainty of \hat{a}_i . To derive uncertainty estimates for causal explanation models, we propose the use of bootstrap ensemble methods, specifically using bootstrap resampling [45, 46]. To train bootstrap ensembles of causal explanation models, we first draw N training samples X at random with repeats from the original training set. We then train an explanation model using the before-mentioned causal objective until convergence on the selected subset of the training set. We repeat this process M times to obtain a bootstrap ensemble of M explanation models (Algorithm in Appendix B). We use the median of the attributions \hat{a}_i of the ensemble members as the assigned importance of the bootstrap ensemble, and the $\frac{\alpha}{2}$ and $1 - \frac{\alpha}{2}$ quantiles as lower and upper bounds of its CI, respectively. The efficacy of bootstrap ensembles for estimating the uncertainty in outputs of neural networks has been demonstrated in, e.g., [47], but this work is, to the best of our knowledge, the first to consider using bootstrap ensembles of explanation models to quantify the uncertainty in assigned importance scores. We note that Monte Carlo dropout [48], which uses dropout [49] at evaluation time, is an alternative method for estimating uncertainty for the outputs of neural networks that does not require explicitly training an ensemble of models, but may not always produce uncertainty estimates of the same quality as ensembles [47].

4 Experiments

Our experiments aimed to answer the following questions:

- 1 How does the feature importance estimation performance of CXPlain compare to that of existing state-of-the-art methods?
- 2 How does the computational performance of CXPlain compare to existing model-agnostic and model-specific methods for feature importance estimation?
- 3 Are uncertainty estimates computed via bootstrap resampling of CXPlain models qualitatively and quantitatively correlated with their ability to accurately determine feature importance?

To answer these questions, we performed extensive experiments on several benchmarks that compare both the computational as well as the estimation performance of CXPlain to existing state-of-the-art methods for feature importance estimation. To enable a meaningful comparison, we focus most of our experiments on image classification tasks, where we are best able to visualise and quantify the performance of feature importance estimation methods, and on neural network models as models to be explained, since most existing model-specific attribution methods that we wish to compare to were developed exclusively for neural networks. However, we note that CXPlain as a method is compatible with any machine-learning model, data modality, and both regression as well as classification tasks. We used Mann–Whitney–Wilcoxon (MWW) tests [50] to calculate p -values for the main comparisons.

4.1 Determining Important Features in MNIST and ImageNet

To compare the accuracy of CXPlain to existing state-of-the-art methods for feature importance estimation, we evaluated its ability to identify important features in MNIST [51] and ImageNet [52] images. To do so, we followed the experimental design first proposed by Shrikumar et al. [1], and

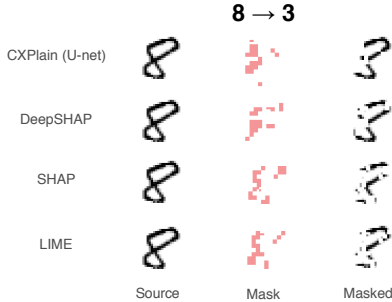


Figure 4: A comparison of the top 10% most important pixels (= Mask) as identified by CXPlain (U-net), DeepSHAP, SHAP, and LIME on the same sample test set image (Source) of the 8 vs. 3 MNIST benchmark. With accurate estimates, the Masked image should more closely resemble a 3 than an 8, since the pixels that most distinguished an 8 as an 8 should have been removed.

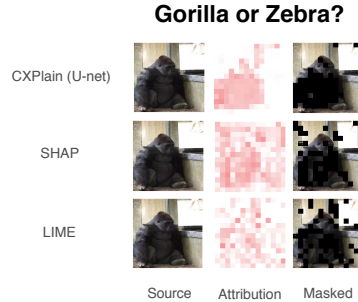


Figure 5: A comparison of the feature importance scores (= Attribution) as estimated by CXPlain (U-net), SHAP, and LIME on the same sample test set image (Source) of the Gorilla vs. Zebra ImageNet benchmark. We found that CXPlain (U-net) produces attribution maps that are, subjectively and qualitatively, more semantically focused on the most salient regions of the image.

trained binary classification models to distinguish between two digit types (8 vs. 3) on MNIST (model accuracy: 99.85%), and two object categories (Gorilla vs. Zebra) on ImageNet (model accuracy: 96.73%). As a preprocessing step, pixel values were scaled to be in the range of $[0, 1]$ prior to training. We then used several importance estimation methods to determine which input pixels were most important for the classification models’ decisions on $N = 100$ test images. We masked the top 10 and 30% of those most important pixels for MNIST and ImageNet, respectively, and measured the resulting change in the classification models’ confidences by computing the difference in log odds

$$\Delta \log\text{-odds} = \log\text{-odds}(p_{\text{original}}) - \log\text{-odds}(p_{\text{masked}}) \quad (7)$$

where $\log\text{-odds}(p) = \log\left(\frac{p}{1-p}\right)$, and p_{original} and p_{masked} are the classification models’ outputs $p \in [0, 1]$ for the original image and the masked image with the top pixels removed, respectively. To ensure that the explanations e_i of all methods are on the same scale, we normalised them to the range of $[0, 1]$ using the transformation $\hat{a}_i = |e_i| / \sum_{i=0}^N |e_i|$. We plotted the assigned importances and the resulting masked images to qualitatively assess each methods’ ability to determine the salient features in the original image (Figures 4 and 5). We additionally recorded the mean and standard deviation of the time taken (in seconds) to compute the feature importance estimates for each method on the same hardware (Appendix C) over 10 and 5 runs with the same parameters and random seed for MNIST and ImageNet, respectively (Figures 6 and 7). Further training details are given in Appendix A.

4.2 Quantifying Uncertainty in Estimates of Feature Importance

To quantitatively and qualitatively assess the accuracy of the uncertainty estimates provided by bootstrap ensembles of CXPlain models, we analysed whether their uncertainty estimates u_i are correlated with their errors in feature importance estimation on held-out MNIST test samples. We evaluated several numbers M of bootstrap resampled models in order to determine how the number of ensemble members affects the uncertainty estimation performance of bootstrap ensembles of CXPlain models. In addition, we also evaluated the performance of randomly selected uncertainty estimates as a baseline for comparison. In general settings, it is difficult to evaluate uncertainty estimates for feature importance estimation methods, since we typically do not have per-feature ground-truth attributions to evaluate against. However, by comparing the ranking implied by the ground-truth change in log-odds to the ranking implied by the explanation model we are able to define a rank error RE_i for each x_i . Formally, the rank error $\text{RE}_i = |\text{rank}_{\Delta \log\text{-odds}}(i) - \text{rank}_{\hat{f}_{\text{exp}}}(i)|$ is the difference in rank between the true rank $\text{rank}_{\Delta \log\text{-odds}}$ implied by $\Delta \log\text{-odds}$, and the estimated rank \hat{f}_{exp} implied by the explanation model, where $\text{rank}_b(i)$ defines the rank of x_i from 0 to $p - 1$ implied by b .

As correlation metric, we used Pearson’s ρ to measure the correlation between the rank error RE_i and the uncertainty estimates $u_i = c_{i,95\%} - c_{i,5\%}$ defined by the bootstrap resampled $\gamma = 90\%$ CIs for each importance estimate \hat{a}_i in the top 2.5% of pixels by $\Delta \log\text{-odds}$ across $N = 100$ unseen images from the MNIST test set. We limited the evaluation to all pixels with a $\Delta \log\text{-odds}$ greater than 0.

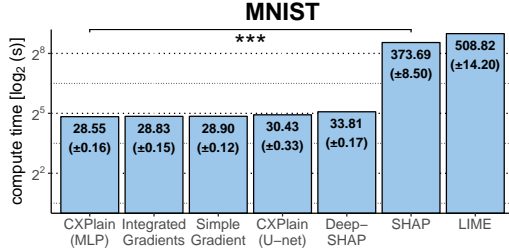


Figure 6: A comparison of the compute time (in \log_2 seconds) needed to produce feature importance estimates using several state-of-the-art feature importance estimation methods on the same hardware for the same $N = 100$ sample test images from the MNIST benchmark (lower is better). *** = significantly different ($p < 0.001$, MWW)

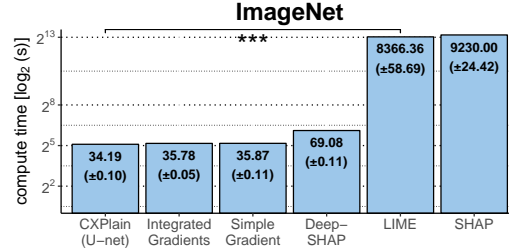


Figure 7: A comparison of the compute time (in \log_2 seconds) needed to produce feature importance estimates using state-of-the-art feature importance estimation methods on the same hardware for the same $N = 100$ sample test images from the ImageNet benchmark (lower is better). *** = significantly different ($p < 0.001$, MWW)

If our uncertainty estimates are well calibrated, we would expect to see a high correlation between the uncertainty estimates u_i and the magnitude of rank errors RE_i , since that would indicate that the uncertainty estimates u_i accurately quantify how certain the feature importance estimates \hat{a}_i are on previously unseen sample images. For the comparison of the resulting distributions of correlation scores, we applied the Fisher z-transform to the correlation scores in order to correct for the skew in the distribution of the sample correlation [53]. Figure 9 depicts visualisations of the calculated ground-truth log odds, the rank errors of the explanation model’s importance estimates, and the uncertainty for each importance estimate for three test set images. We used the same hyperparameters as in the previous experiment to train the ensembled CXPlain (MLP) models (Appendix A).

5 Results and Discussion

Predictive Performance. We found that, on the MNIST benchmark, CXPlain (U-net) was competitive with the best competing state-of-the-art feature importance estimation method, DeepSHAP. We also found that CXPlain (U-net) produced significantly ($p < 0.001$, MWW) more accurate feature importance estimates than CXPlain (MLP) - indicating that model architectures specifically tailored for the image domain are more effective than MLPs in neural explanation models (Figure 2). On the ImageNet benchmark, CXPlain significantly ($p < 0.01$, MWW) outperformed the best competing feature importance estimation method, LIME (Figure 3). We also found that the model-specific attribution methods Simple Gradient and Integrated Gradients performed relatively poorly across both benchmarks, and were consistently outperformed by the model-agnostic attribution methods, CXPlain, and DeepSHAP. Qualitatively, we found that the estimates of feature importance provided by CXPlain were more focused on the subjectively more important semantic regions of the sample images from both MNIST and ImageNet (Figures 4 and 5; more in Appendix D). Other methods, in contrast, produced more superfluous attributions. This behavior is exhibited in Figure 5 where SHAP and LIME both attribute significant importance to the wall behind the gorilla, whereas CXPlain focused nearly all its attention on the gorilla itself, with the exception of the window frame receiving some importance outside the top 30% of importances of that sample image. We believe this could be due to the fact that the causal objective strongly penalises attributions outside regions of interest - leading to qualitatively more focused estimates of importance.

Computational Performance. In terms of computational performance, we found that CXPlain computed feature importance estimates significantly faster than the state-of-the-art model-agnostic attribution methods, LIME and SHAP, on both the MNIST and ImageNet benchmarks (Figures 6 and 7). Gradient-based attribution methods and CXPlain performed similarly. On ImageNet, the gap between LIME and SHAP and the faster methods was considerably larger than on MNIST, since the large numbers of model evaluations for LIME and SHAP were slower on higher-dimensional images.

Quality of Uncertainty Estimates. We found that, quantitatively, even relatively small CXPlain ensembles with just $M = 5$ bootstrap resampled models produce uncertainty estimates that are significantly ($p < 0.001$, MWW, compared to Random) correlated with its ability to accurately estimate feature importances on $N = 100$ previously unseen test images (Figure 8). We also found

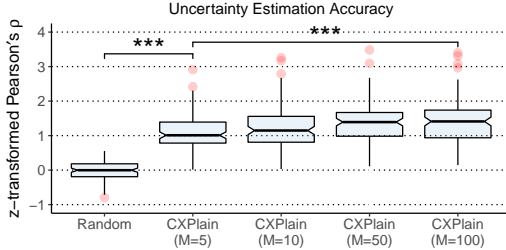


Figure 8: A comparison of the distributions of the z-transformed Pearson’s correlations ρ between the uncertainty estimates u_i produced by various numbers M of bootstrapped ensembles of CXPlain models and the Random baseline, and the ground-truth rank errors of the top 2.5% most important pixels across $N = 100$ unseen test images from the MNIST benchmark (higher is better). *** = significantly different ($p < 0.001$, MWW)

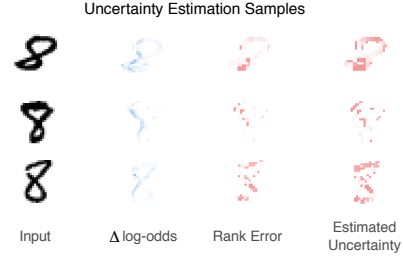


Figure 9: Visualisations of the calculated ground-truth change in log odds $\Delta \log\text{-odds}$, the Rank Errors of the explanation model’s feature importance estimates, and the Estimated Uncertainty for each feature importance estimate as obtained via bootstrap resampling ($M = 100$) for three unseen sample test set images (Input) from the MNIST benchmark. Note the visual similarity of the Rank Error and the Estimated Uncertainty.

that increasing the size M of the bootstrap ensemble further significantly ($p < 0.001$ for $M = 5$ to $M = 100$, MWW) increases this correlation, and, thus, the quality of the provided uncertainty estimates. Qualitatively, there was a high visual similarity between the uncertainty estimates u_i provided by the CXPlain ensembles for each input feature x_i and the magnitude of rank errors RE_i committed by its importance estimates \hat{a}_i (Figure 9). The large differences in importance estimation accuracy between state-of-the-art feature importance estimation methods shown in the MNIST and ImageNet benchmarks indicate that many of the importance estimates they provide are not truthful to the predictive model \hat{f} to be explained, and that measures of uncertainty are necessary to fully understand the expected reliability of feature importance estimates.

Limitations. While they are fast at evaluation time, a limitation of CXPlain models is that they have to be trained to learn to explain a predictive model. However, this one-off compute cost typically amortises quickly, since CXPlain is significantly faster at evaluation time than existing model-agnostic importance estimation methods. Another important point to note is that the associations identified by CXPlain models are only causal in the sense that they quantify the degree to which the input features x_i caused a marginal improvement in the predictive performance of the predictive model \hat{f} . Associations reported by CXPlain, in particular, do not in any way indicate that there is a causal relationship between the explained model’s input and output variables in the real world.

6 Conclusion

We presented CXPlain, a new method for learning to estimate feature importance for any machine-learning model. CXPlain is based on the idea of training a separate explanation model to learn to estimate which features are important for a given output of a target predictive model using a causal objective. This approach has several advantages over existing ones: It is compatible with any machine-learning model, can produce estimates of feature importance quickly after training, and may be combined with bootstrap resampling to obtain uncertainty estimates for the provided feature importance scores. We showed experimentally that CXPlain is significantly more accurate in estimating feature importance than existing model-agnostic methods on both MNIST and ImageNet benchmarks, while being orders of magnitude faster at providing importance estimates than state-of-the-art model-agnostic methods. We also found that, analogous to standard supervised learning tasks, special-purpose model architectures may improve the performance of neural explanation models in images, and that the bootstrap resampled uncertainty estimates for the importance scores of an explanation model are significantly correlated with CXPlain’s ability to accurately estimate feature importance - indicating that bootstrap resampling is a suitable approach for quantifying the uncertainty of importance estimates. Causal explanation models that both produce accurate estimates of feature importance and their uncertainties quickly for any machine-learning model and data modality may enable users to better understand, validate, and interpret machine-learning models, while also informing them when their explanations can not be expected to be accurate.

Acknowledgments

This work was partially funded by the Swiss National Science Foundation (SNSF) project No. 167302 within the National Research Program (NRP) 75 “Big Data”. We gratefully acknowledge the support of NVIDIA Corporation with the donation of the Titan Xp GPUs used for this research. Patrick Schwab is an affiliated PhD fellow at the Max Planck ETH Center for Learning Systems. We additionally thank the anonymous reviewers whose comments helped improve this manuscript.

References

- [1] Avanti Shrikumar, Peyton Greenside, Anna Shcherbina, and Anshul Kundaje. Learning important features through propagating activation differences. *International Conference of Machine Learning*, 2017.
- [2] Zachary C Lipton. The mythos of model interpretability. *arXiv preprint arXiv:1606.03490*, 2016.
- [3] Pieter-Jan Kindermans, Sara Hooker, Julius Adebayo, Maximilian Alber, Kristof T Schütt, Sven Dähne, Dumitru Erhan, and Been Kim. The (un) reliability of saliency methods. *arXiv preprint arXiv:1711.00867*, 2017.
- [4] Daniel Smilkov, Nikhil Thorat, Been Kim, Fernanda Viégas, and Martin Wattenberg. Smoothgrad: removing noise by adding noise. *arXiv preprint arXiv:1706.03825*, 2017.
- [5] Finale Doshi-Velez and Been Kim. Towards a rigorous science of interpretable machine learning. *arXiv preprint arXiv:1702.08608*, 2017.
- [6] Scott M Lundberg and Su-In Lee. A unified approach to interpreting model predictions. In *Advances in Neural Information Processing Systems*, pages 4768–4777, 2017.
- [7] David Baehrens, Timon Schroeter, Stefan Harmeling, Motoaki Kawanabe, Katja Hansen, and Klaus-Robert Müller. How to explain individual classification decisions. *Journal of Machine Learning Research*, 11 (Jun):1803–1831, 2010.
- [8] Karen Simonyan, Andrea Vedaldi, and Andrew Zisserman. Deep inside convolutional networks: Visualising image classification models and saliency maps. *International Conference on Learning Representations*, 2014.
- [9] Matthew D Zeiler and Rob Fergus. Visualizing and understanding convolutional networks. In *European Conference on Computer Vision*, pages 818–833. Springer, 2014.
- [10] Mukund Sundararajan, Ankur Taly, and Qiqi Yan. Axiomatic attribution for deep networks. *International Conference on Machine Learning*, 2017.
- [11] Kelvin Xu, Jimmy Ba, Ryan Kiros, Kyunghyun Cho, Aaron Courville, Ruslan Salakhudinov, Rich Zemel, and Yoshua Bengio. Show, attend and tell: Neural image caption generation with visual attention. In *International Conference on Machine Learning*, pages 2048–2057, 2015.
- [12] Edward Choi, Mohammad Taha Bahadori, Jimeng Sun, Joshua Kulas, Andy Schuetz, and Walter Stewart. Retain: An interpretable predictive model for healthcare using reverse time attention mechanism. In *Advances in Neural Information Processing Systems*, pages 3504–3512, 2016.
- [13] Patrick Schwab, Gaetano C. Scebba, Jia Zhang, Marco Delai, and Walter Karlen. Beat by Beat: Classifying Cardiac Arrhythmias with Recurrent Neural Networks. In *Computing in Cardiology*, 2017.
- [14] Patrick Schwab, Djordje Miladinovic, and Walter Karlen. Granger-causal Attentive Mixtures of Experts: Learning Important Features with Neural Networks. In *AAAI Conference on Artificial Intelligence*, 2019.
- [15] Patrick Schwab and Walter Karlen. PhoneMD: Learning to diagnose Parkinson’s disease from smartphone data. In *AAAI Conference on Artificial Intelligence*, 2019.
- [16] Marco Tulio Ribeiro, Sameer Singh, and Carlos Guestrin. Why should i trust you?: Explaining the predictions of any classifier. In *Proceedings of the 22nd ACM SIGKDD International Conference on Knowledge Discovery and Data Mining*, pages 1135–1144. ACM, 2016.
- [17] Julius Adebayo, Justin Gilmer, Michael Muellly, Ian Goodfellow, Moritz Hardt, and Been Kim. Sanity checks for saliency maps. In *Advances in Neural Information Processing Systems*, pages 9505–9515, 2018.
- [18] Hui Fen, Kuangyan Song, Madeilene Udell, Yiming Sun, Yujia Zhang, et al. Why should you trust my interpretation? Understanding uncertainty in LIME predictions. *arXiv preprint arXiv:1904.12991*, 2019.

- [19] Amirata Ghorbani, Abubakar Abid, and James Zou. Interpretation of neural networks is fragile. *AAAI Conference on Artificial Intelligence*, 2019.
- [20] Erik Štrumbelj, Igor Kononenko, and M Robnik Šikonja. Explaining instance classifications with interactions of subsets of feature values. *Data & Knowledge Engineering*, 68(10):886–904, 2009.
- [21] Luisa M Zintgraf, Taco S Cohen, Tameem Adel, and Max Welling. Visualizing deep neural network decisions: Prediction difference analysis. In *International Conference on Learning Representations*, 2017.
- [22] Jiwei Li, Will Monroe, and Dan Jurafsky. Understanding neural networks through representation erasure. *arXiv preprint arXiv:1612.08220*, 2016.
- [23] Ruth C Fong and Andrea Vedaldi. Interpretable explanations of black boxes by meaningful perturbation. In *IEEE International Conference on Computer Vision*, 2017.
- [24] Piotr Dabkowski and Yarin Gal. Real time image saliency for black box classifiers. In *Advances in Neural Information Processing Systems*, pages 6967–6976, 2017.
- [25] Patrick Schwab and Helmut Hlavacs. Capturing the essence: Towards the automated generation of transparent behavior models. In *AAAI Conference on Artificial Intelligence and Interactive Digital Entertainment*, 2015.
- [26] Zhengping Che, Sanjay Purushotham, Robinder Khemani, and Yan Liu. Interpretable deep models for ICU outcome prediction. In *AMIA Annual Symposium Proceedings*, volume 2016, page 371. American Medical Informatics Association, 2016.
- [27] Osbert Bastani, Carolyn Kim, and Hamsa Bastani. Interpreting blackbox models via model extraction. *arXiv preprint arXiv:1705.08504*, 2017.
- [28] Robert Andrews, Joachim Diederich, and Alan B Tickle. Survey and critique of techniques for extracting rules from trained artificial neural networks. *Knowledge-based Systems*, 8(6):373–389, 1995.
- [29] Aditya Chattopadhyay, Piyushi Manupriya, Anirban Sarkar, and Vineeth N Balasubramanian. Neural network attributions: A causal perspective. *arXiv preprint arXiv:1902.02302*, 2019.
- [30] Grégoire Montavon, Sebastian Lapuschkin, Alexander Binder, Wojciech Samek, and Klaus-Robert Müller. Explaining nonlinear classification decisions with deep taylor decomposition. *Pattern Recognition*, 65: 211–222, 2017.
- [31] Jianbo Chen, Le Song, Martin J Wainwright, and Michael I Jordan. Learning to explain: An information-theoretic perspective on model interpretation. *International Conference on Machine Learning*, 2018.
- [32] Wenbo Guo, Sui Huang, Yunzhe Tao, Xinyu Xing, and Lin Lin. Explaining deep learning models—a bayesian non-parametric approach. In *Advances in Neural Information Processing Systems*, pages 4514–4524, 2018.
- [33] Michael Tsang, Dehua Cheng, and Yan Liu. Detecting statistical interactions from neural network weights. *International Conference on Learning Representations*, 2017.
- [34] Been Kim, Martin Wattenberg, Justin Gilmer, Carrie Cai, James Wexler, Fernanda Viegas, and Rory Sayres. Interpretability beyond feature attribution: Quantitative testing with concept activation vectors (TCAV). *International Conference on Machine Learning*, 2018.
- [35] Pang Wei Koh and Percy Liang. Understanding black-box predictions via influence functions. *International Conference of Machine Learning*, 2017.
- [36] Clive WJ Granger. Investigating causal relations by econometric models and cross-spectral methods. *Econometrica: Journal of the Econometric Society*, pages 424–438, 1969.
- [37] Richard Stone. The assumptions on which causal inferences rest. *Journal of the Royal Statistical Society. Series B (Methodological)*, pages 455–466, 1993.
- [38] Dominik Janzing, David Balduzzi, Moritz Grosse-Wentrup, and Bernhard Schölkopf. Quantifying causal influences. *The Annals of Statistics*, 41(5):2324–2358, 2013.
- [39] Pasha Khosravi, Yitao Liang, YooJung Choi, and Guy Van den Broeck. What to expect of classifiers? Reasoning about logistic regression with missing features. *arXiv preprint arXiv:1903.01620*, 2019.
- [40] Solomon Kullback. *Information theory and statistics*. Courier Corporation, 1997.

- [41] Ian Goodfellow, Yoshua Bengio, and Aaron Courville. *Deep learning*. MIT Press, 2016.
- [42] Christian Szegedy, Vincent Vanhoucke, Sergey Ioffe, Jon Shlens, and Zbigniew Wojna. Rethinking the Inception architecture for computer vision. In *IEEE Conference on Computer Vision and Pattern Recognition*, pages 2818–2826, 2016.
- [43] Lukasz Kaiser, Aidan N Gomez, Noam Shazeer, Ashish Vaswani, Niki Parmar, Llion Jones, and Jakob Uszkoreit. One Model To Learn Them All. *arXiv preprint arXiv:1706.05137*, 2017.
- [44] Olaf Ronneberger, Philipp Fischer, and Thomas Brox. U-net: Convolutional networks for biomedical image segmentation. In *International Conference on Medical Image Computing and Computer-assisted Intervention*, pages 234–241. Springer, 2015.
- [45] Bradley Efron. *The jackknife, the bootstrap, and other resampling plans*, volume 38. Siam, 1982.
- [46] Leo Breiman. Random forests. *Machine Learning*, 45(1):5–32, 2001.
- [47] Balaji Lakshminarayanan, Alexander Pritzel, and Charles Blundell. Simple and scalable predictive uncertainty estimation using deep ensembles. In *Advances in Neural Information Processing Systems*, pages 6402–6413, 2017.
- [48] Yarín Gal and Zoubin Ghahramani. Dropout as a Bayesian approximation: Representing model uncertainty in deep learning. In *International Conference on Machine Learning*, pages 1050–1059, 2016.
- [49] Nitish Srivastava, Geoffrey Hinton, Alex Krizhevsky, Ilya Sutskever, and Ruslan Salakhutdinov. Dropout: A simple way to prevent neural networks from overfitting. *The Journal of Machine Learning Research*, 15(1):1929–1958, 2014.
- [50] Myles Hollander and Douglas A Wolfe. *Nonparametric statistical methods*. Wiley New York, NY, USA, 1973.
- [51] Yann LeCun, Corinna Cortes, and CJ Burges. MNIST handwritten digit database. *AT&T Labs [Online]*. Available: <http://yann.lecun.com/exdb/mnist>, 2:18, 2010.
- [52] Jia Deng, Wei Dong, Richard Socher, Li-Jia Li, Kai Li, and Li Fei-Fei. Imagenet: A large-scale hierarchical image database. In *IEEE Conference on Computer Vision and Pattern Recognition*, pages 248–255. IEEE, 2009.
- [53] N Clayton Silver and William P Dunlap. Averaging correlation coefficients: Should Fisher’s z transformation be used? *Journal of Applied Psychology*, 72(1):146, 1987.
- [54] Martín Abadi, Ashish Agarwal, Paul Barham, Eugene Brevdo, Zhifeng Chen, Craig Citro, Greg S Corrado, Andy Davis, Jeffrey Dean, Matthieu Devin, et al. Tensorflow: Large-scale machine learning on heterogeneous distributed systems. *arXiv preprint arXiv:1603.04467*, 2016.
- [55] Sergey Ioffe and Christian Szegedy. Batch normalization: Accelerating deep network training by reducing internal covariate shift. In *International Conference on Machine Learning*, pages 448–456, 2015.
- [56] Diederik Kingma and Jimmy Ba. Adam: A method for stochastic optimization. In *International Conference on Learning Representations*, 2015.
- [57] Günter Klambauer, Thomas Unterthiner, Andreas Mayr, and Sepp Hochreiter. Self-normalizing neural networks. In *Advances in Neural Information Processing Systems*, pages 971–980, 2017.

Supplementary Material for: "CXPlain: Causal Explanations for Model Interpretation under Uncertainty"

Patrick Schwab and Walter Karlen
Institute of Robotics and Intelligent Systems, ETH Zurich
patrick.schwab@hest.ethz.ch

A Hyperparameters

We implemented all our experiments using Python and TensorFlow [52], and used standardised compute hardware to run the experiments (see Appendix C). For both benchmarks, we used 10000 perturbed samples per explained image for both LIME and SHAP. The output layer of all CXPlain models had one output node for each of the p output feature importance scores a_i , and was followed by a softmax activation. We used reference implementations provided by the method's original authors for LIME¹, SHAP and DeepSHAP², and our own implementations for Simple Gradient and Integrated Gradients. To keep the computation time for sensitivity-based attribution methods in a reasonable range, we explain non-overlapping connected regions of 2x2 pixels for the MNIST benchmarks, and regions of 16x16 pixels for the ImageNet benchmarks. Since the image dimensions were 28x28 for MNIST and 224x224 for ImageNet, the target attribution maps were of size 14x14 for both benchmarks. To keep the comparison meaningful, we summed and renormalised the attributions for each block for the methods that produced per-pixel importances to downsample their attribution maps to the same resolution. For CXPlain, we also used a target attribution map size of 14x14. For the ImageNet benchmark, we split the dataset at random stratified by class into training (60%), validation (20%), and test set (20% of all samples). For MNIST, we used the splits from [49].

MNIST Benchmark. As target predictive model, we used a binary classifier ResNet-20 model using rectified linear (ReLU) units without batch normalisation [53] that was trained with the Adam [54] optimiser, a learning rate of 0.001, weight decay of 0.001, a batch size of 32, for a maximum of 50 epochs and an early stopping patience of 12 on the validation set loss, and achieved a test set accuracy of 99.85% in distinguishing between the two digit classes. The CXPlain (MLP) model was trained with the Adam [54] optimiser, a learning rate of 0.001, a batch size of 100, 2 hidden layers, H hidden units per hidden layer each followed by a scaled exponential linear unit (SELU) activation [55], for a maximum of 50 epochs with an early stopping patience of 12 on the validation set loss. The CXPlain (U-net) model was trained with the Adam [54] optimiser for a maximum of 50 epochs with an early stopping patience of 12 on the validation set loss, a learning rate of 0.002, a batch size of 128, K filters in the first convolutional layer and $K * 2^{\text{layer_index}}$ filters in every subsequent pair of convolutional layer for a maximum of 2 pairs of convolutional layers in the first stage of the U-net followed by a max pooling operation that reduced the dimensionality of the layer input both in width and height in half. The same steps were then mirrored in the inverse direction as outlined in [41] until the target attribution map dimension of $14 * 14$ was reached. Each convolutional layer was followed by a ReLU activation. We used a total of 5 hyperparameter optimisation runs on the validation set to select the number H of hidden units per hidden layer of the CXPlain (MLP) model, the number K of initial convolutional filters of the CXPlain (U-net) model, and the dropout probability of both at random from predefined ranges (Tables S1 and S2). The CXPlain (MLP) model selected after

¹<https://github.com/marcotcr/lime>

²<https://github.com/slundberg/shap>

hyperparameter optimisation used a dropout rate of 4.01%, 126 hidden units per hidden layer, and was trained in 288.73 seconds after precomputing Ω for each sample X . The CXPlain (U-net) model selected after hyperparameter optimisation used a dropout rate of 0.001%, 77 initial convolutional filters, and was trained in 499.38 seconds after precomputing Ω for each sample X . We used the digits 8 and 3 for the MNIST benchmark.

ImageNet Benchmark. As target predictive model, we used a binary classifier ResNet-32 model using rectified linear (ReLU) units without batch normalisation [53] that was trained with the Adam [54] optimiser, a learning rate of 0.01, a batch size of 32, for a maximum of 250 epochs and an early stopping patience of 12 on the validation set loss, and achieved a test set accuracy of 96.73% in distinguishing between the two object classes. During training, we used automated data augmentation that transformed the image with a randomised shear, zoom, width shift, and height shift of up to 10%, rotated the image at most 20 degrees and flipped the images horizontally at random. The CXPlain (U-net) model was trained with the Adam [54] optimiser, a learning rate of 0.001, a batch size of 32, K filters in the first convolutional layer and $K * 2^{\text{layer_index}}$ filters in every subsequent pair of convolutional layer for a maximum of 5 pairs of convolutional layers in the first stage of the U-net followed by a max pooling operation that reduced the dimensionality of the layer input both in width and height in half. The same steps were then mirrored in the inverse direction as outlined in [41]. Each convolutional layer was followed by a ReLU activation. We used a total of 5 hyperparameter optimisation runs on the validation set to select the number K of initial convolutional filters and dropout probability of the CXPlain (U-net) model at random from predefined ranges (Table S3). The CXPlain (U-net) model selected after hyperparameter optimisation used a dropout rate of 5.61%, 12 initial convolutional filters, and was trained in 372.14 seconds after precomputing Ω for each sample X . The ImageNet synsets we used for the benchmark were zebra (n02391049) and gorilla (n02480855).

Twitter Sentiment Analysis Benchmark. In addition to the benchmarks presented in the main body of the paper, we also performed qualitative experiments using a sentiment analysis model for short text messages in order to demonstrate the efficacy of CXPlain for data modalities other than images, and target predictive models other than neural networks. As training dataset, we used a random subset of $N = 100000$ short messages (50000 positive and 50000 negative messages) from the dataset available at <http://cs.stanford.edu/people/alecmgo/trainingandtestdata.zip>. Like the ImageNet benchmark, we split the dataset at random stratified by class into training (60%), validation (20%), and test set (20% of all samples). We then trained a random forest (RF) classifier with 64 trees to classify short messages as being either positive or negative in content as our target predictive model. The model achieved a test set accuracy of 76.32%. The RF model received word count vectors over a vocabulary initialised with the training set as inputs. The input text was lowercased, punctuation was removed, and the words were preprocessed using the Natural Language Toolkit (NLTK) tokeniser available at <https://www.nltk.org/>. As explanation model, we trained a CXPlain (MLP) model that received a fixed length sequence of 96 word IDs according to the previously mentioned vocabulary in order to determine which words were most important for the RFs outputs. Messages shorter than 96 were padded with the zero ID that was not assigned to any other words, and words that were not in the training vocabulary were assigned an ID representing unknown words that was not assigned to any other words. The CXPlain (MLP) used an initial embedding layer to transform the word IDs into an embedding space that was followed by a number of L hidden layers with H hidden units each. Each layer was followed by a SeLU activation [55]. The CXPlain (MLP) model was trained with the Adam [54] optimiser, a learning rate of 0.0001, a batch size of 128, and a dropout percentage p_{dropout} for a maximum of 100 epochs and an early stopping patience of 12 on the validation set loss. H , L and p_{dropout} were selected at random from predefined ranges over 5 hyperparameter optimisation runs using the lowest validation loss as the selection criterium (Table S4). The CXPlain (MLP) model selected after hyperparameter optimisation used a dropout rate of 5.47%, 162 hidden units per hidden layer, 1 hidden layer, and was trained in 126.28 seconds after precomputing Ω for each sample X . To remove the information from the i th word x_i for the calculation of the causal objective, we simply deleted the respective word from the sentence. See Appendix E for qualitative samples of importances assigned by the selected CXPlain (MLP) to short text messages from the Twitter Sentiment Analysis benchmark.

B Training Bootstrap Ensembles of Causal Explanation Models

Algorithm 1 Training Bootstrap Ensembles of Causal Explanation Models.

Input:

- 1: Training dataset T consisting of N samples X with ground-truth labels y
- 2: Size M of ensemble
- 3: Target predictive model \hat{f} to be explained

Output: Ensemble E of M causal explanation models

- 4: **procedure** TRAIN_EXPLANATION_ENSEMBLE:
 - 5: $E \leftarrow$ Empty
 - 6: **for** i from 0 to $M - 1$ **do**
 - 7: $T_{\text{subset}} \leftarrow$ Draw N pairs of samples (X, y) at random with repeats from T
 - 8: Train explanation model CXPlain_i until convergence using $\mathcal{L}_{\text{causal}}$ with \hat{f} and T_{subset} .
 - 9: Add CXPlain_i to E
 - return** E
-

C Computing Infrastructure

We used the same hardware for all experiments: Intel Core i5 7600K, Nvidia GeForce Titan Xp, 32 GB RAM.

D Qualitative Samples for the MNIST and ImageNet Benchmarks

We present more qualitative samples from the MNIST benchmark in Figure S1, and more qualitative samples from the ImageNet benchmark in Figure S2.

E Qualitative Samples for the Twitter Sentiment Analysis Benchmark

We show qualitative samples of the importances assigned to short messages in the Twitter Sentiment Analysis benchmark by the CXPlain (MLP) in Table S5. We found that, qualitatively, the explanations of CXPlain (MLP) provided for the RF were indeed high for words that have positive or negative connotations, and, subjectively, appeared to be semantically meaningful.

Table S1: Hyperparameter ranges used to train CXPlain (MLP) in the MNIST benchmark.

Hyperparameter	Values
Number of hidden units per hidden layer H	[70, 140]
Dropout percentage p_{dropout}	[0%, 10%]

Table S2: Hyperparameter ranges used to train CXPlain (U-net) in the MNIST benchmark.

Hyperparameter	Values
Number of initial convolutional filters K	[65, 80]
Dropout percentage p_{dropout}	[0%, 10%]

Table S3: Hyperparameter ranges used to train CXPlain (U-net) in the ImageNet benchmark.

Hyperparameter	Values
Number of initial convolutional filters K	[8, 24]
Dropout percentage p_{dropout}	[0%, 10%]

Table S4: Hyperparameter ranges used to train CXPlain (MLP) in the Sentiment Analysis benchmark.

Hyperparameter	Values
Number of hidden units per hidden layer H	[64, 180]
Number of hidden layers L	[1, 3]
Dropout percentage p_{dropout}	[0%, 10%]

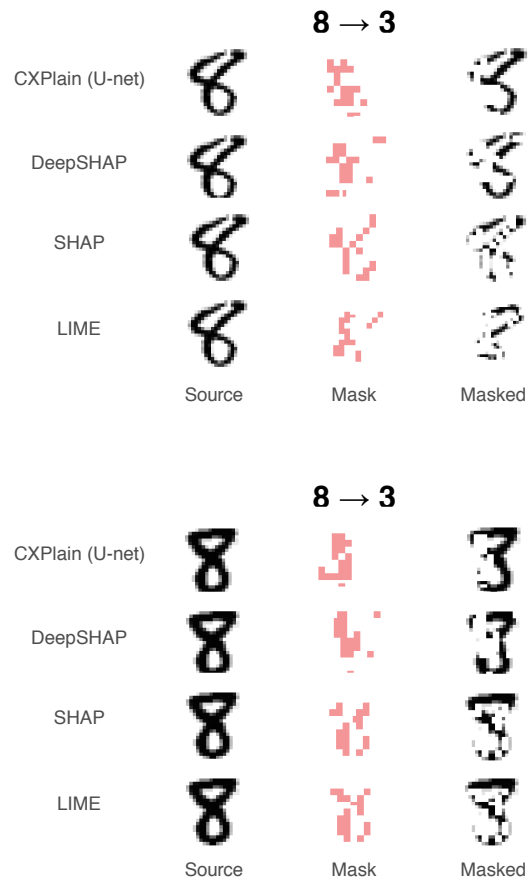
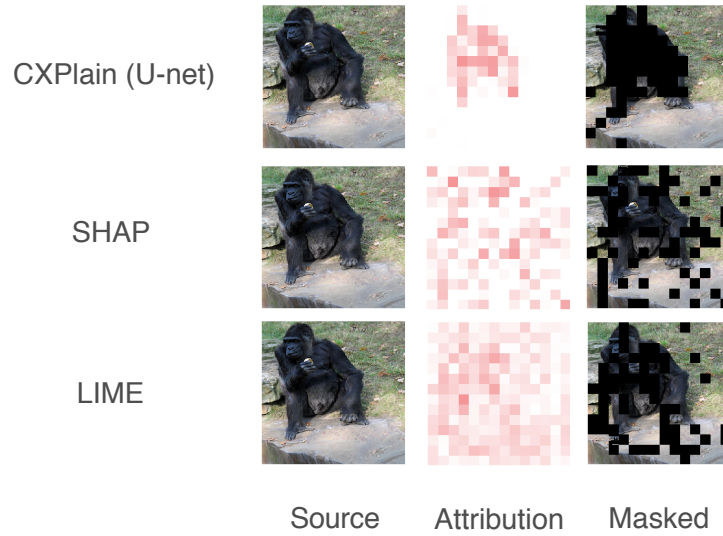


Figure S1: Additional qualitative comparisons of the top 10% most important pixels (= Mask) as identified by CXPlain (U-net), DeepSHAP, SHAP, and LIME on two sample test set images (Source) of the 8 vs. 3 MNIST benchmark.

Gorilla or Zebra?



Gorilla or Zebra?

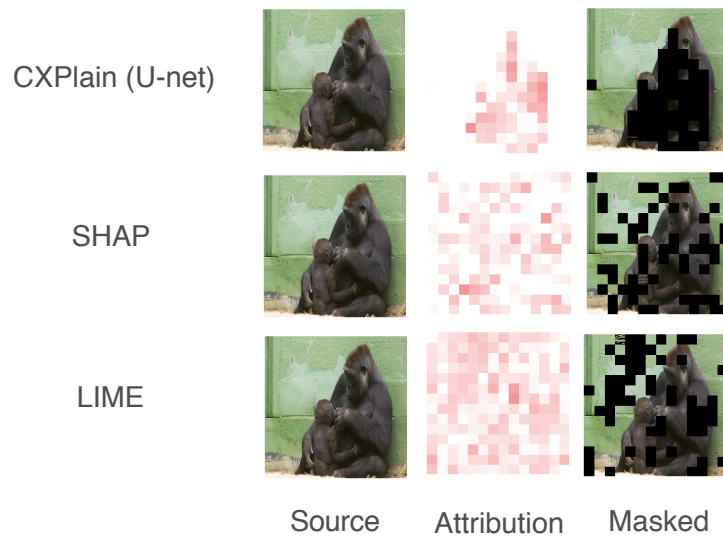


Figure S2: Additional qualitative comparisons of feature importance scores (= Attribution) as estimated by CXPlain (U-net), SHAP, and LIME on two same sample test set images (Source) of the Gorilla vs. Zebra ImageNet benchmark.

Table S5: Examples of short messages and the importances assigned by CXPlain (MLP) in the Twitter Sentiment Analysis benchmark. Deeper colors indicate higher importances, as indicated in the labelled examples in the header row of the table. All samples are labelled as positive in sentiment.

Short messages	highest importance	lowest importance
you re welcome glad you enjoyed it		
is awesome thanks got some good lolz needed it xxx		
today its already busy i wish it was slow maybe later hopefully		
whoooooo finally done with high school thank god just graduation now yay		
happy emox awe i d be sad if you bear napped him		
thank you all so much for your kindness		
bout half way done packing gon na be a long ride thanks for the sketch hanna		
thanks for all the gr follows in the last hrs i m awed with each of you		
what are yall doing in the lb you guys should kick it at my place		
looking forward to his birthday tomorrow		